

## Electronic Supplementary Information

**Large mass field fluctuation and lattice anharmonicity effects promote thermoelectric and mechanical performances in NbFeSb half-Heusler alloys via Ti/Zr/Hf stepwise doping**

Chang Tan,<sup>a</sup> Hongxiang Wang,<sup>a</sup> Lingwen Zhao,<sup>a</sup> Yuqing Sun,<sup>a</sup> Jie Yao,<sup>a</sup> Jinze Zhai,<sup>a</sup>  
Chunlei Wang,<sup>a</sup> Hongchao Wang<sup>a\*</sup>

<sup>a</sup>School of Physics, State Key Laboratory of Crystal Materials, Shandong University,  
Jinan, 250100, PR China

\*Correspondence: wanghc@sdu.edu.cn (H. Wang)

## Supplementary Figures

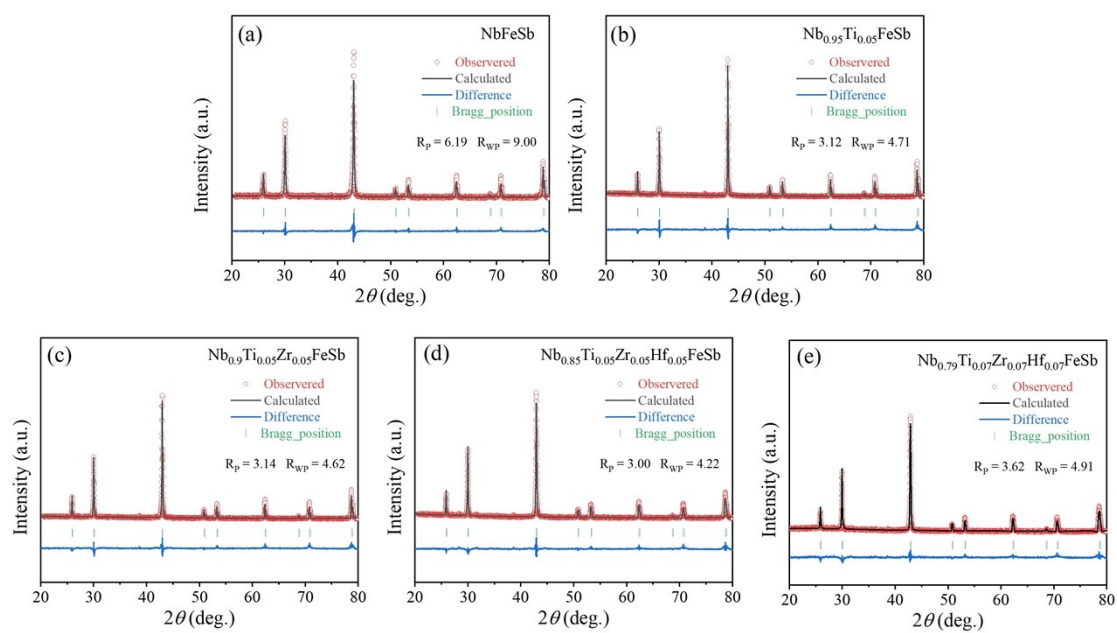


**Fig. S1.** Rietveld refinement result of the  $\text{Nb}_{1-x-y-z}\text{Ti}_x\text{Zr}_y\text{Hf}_z\text{FeSb}$  ( $x, y, z = 0, 0.05, 0.07$ ) sample.

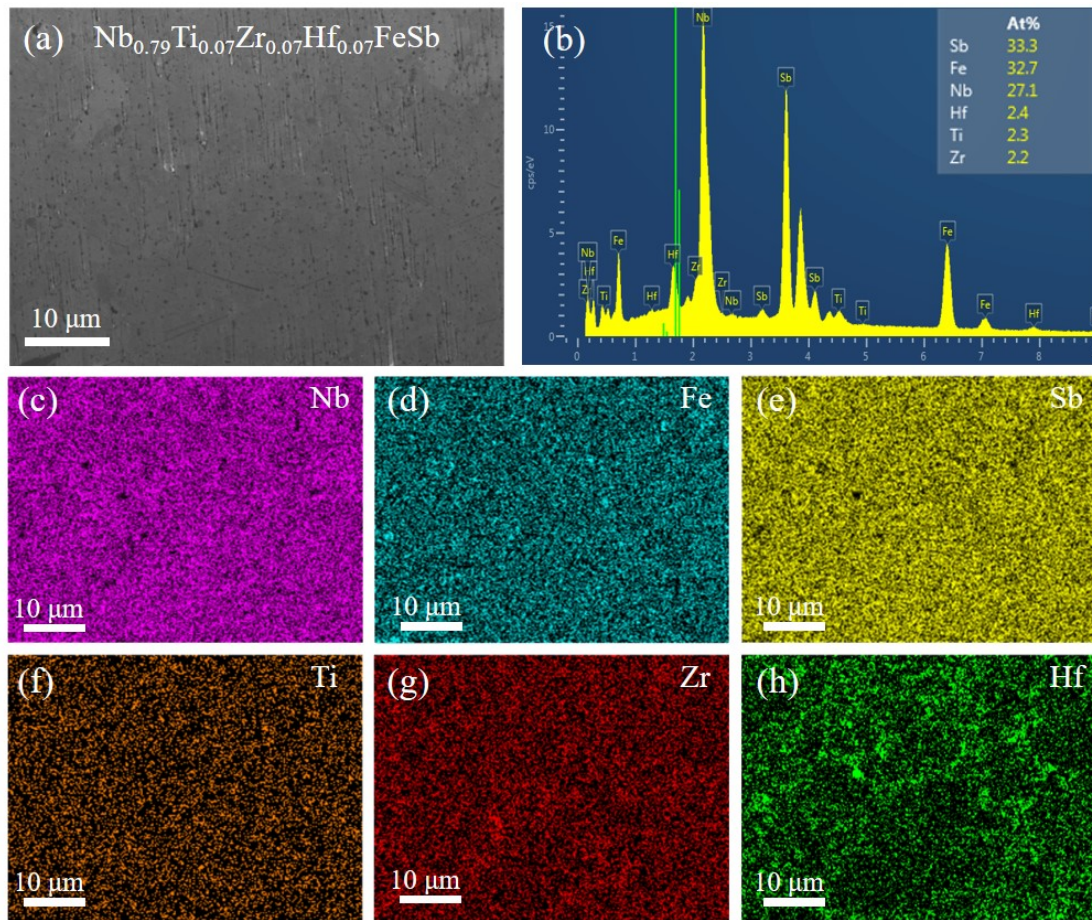


**Fig. S2.** (a) Scanning electron microscopy (SEM) image of a polished surface of the  $\text{Nb}_{0.79}\text{Ti}_{0.07}\text{Zr}_{0.07}\text{Hf}_{0.07}\text{FeSb}$  sample. (b) Corresponding energy dispersive spectrometry (EDS) and mappings of (c) Nb, (d) Fe, (e) Sb, (f) Ti, (g) Zr, (h) Hf.

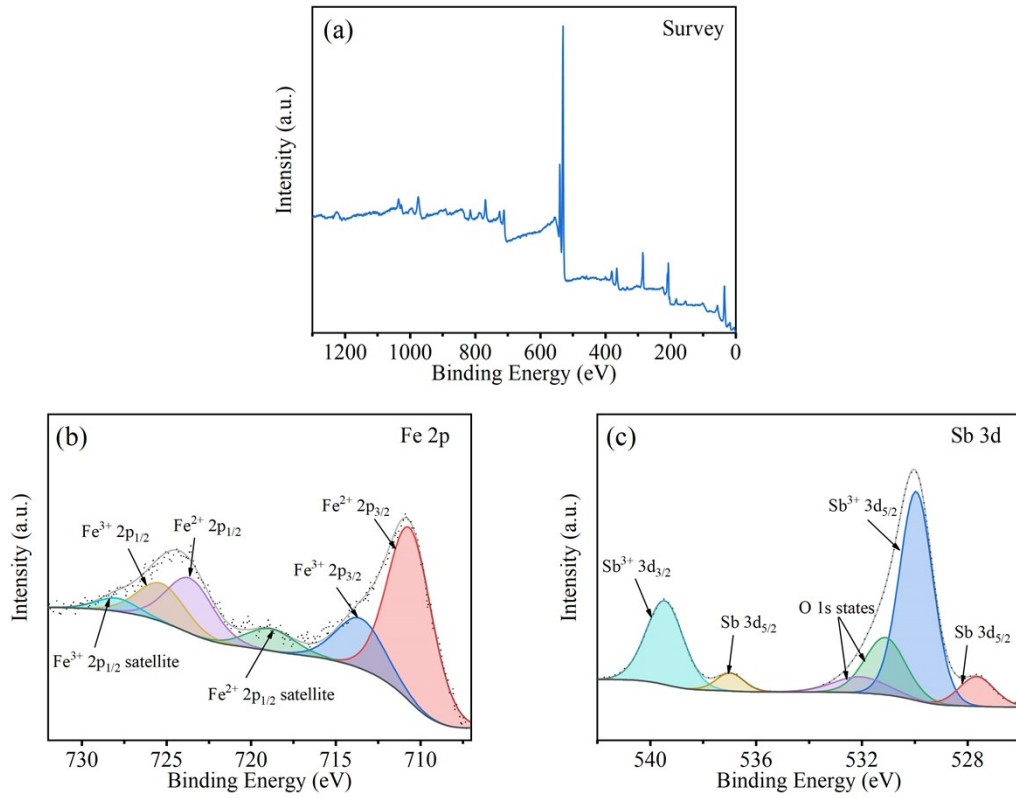


**Fig. S3.** X-ray photoelectron spectra (XPS) of the  $\text{Nb}_{0.82}\text{Ti}_{0.06}\text{Zr}_{0.06}\text{Hf}_{0.06}\text{FeSb}$  sample for (a) full spectrum, (b) Fe 2p, (c) Sb 3d.

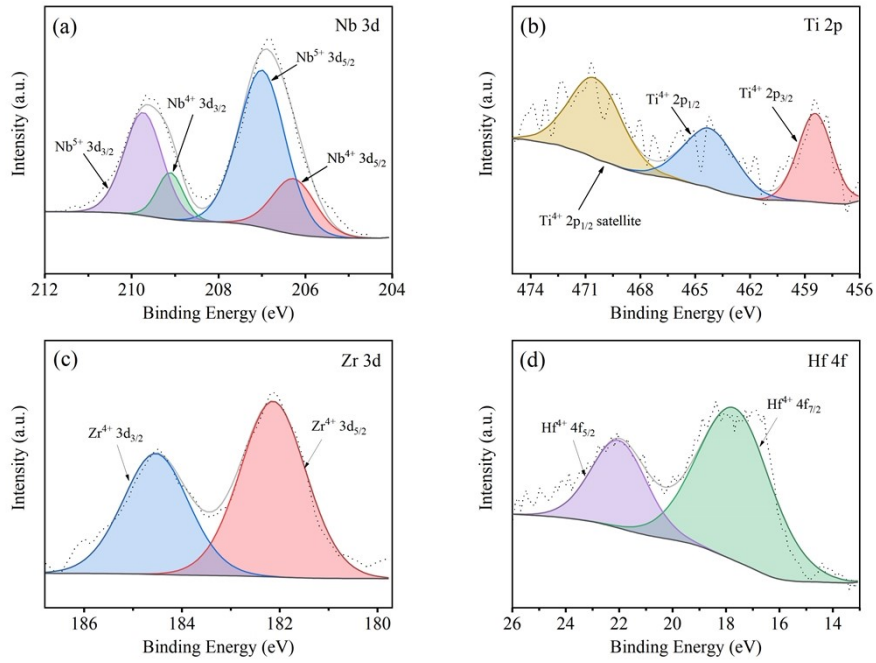


**Fig S4.** X-ray photoelectron spectra (XPS) of the  $\text{Nb}_{0.82}\text{Ti}_{0.06}\text{Zr}_{0.06}\text{Hf}_{0.06}\text{FeSb}$  sample for (a) Nb 3d, (b) Ti 2p, (c) Zr 3d, (d) Hf 4f.

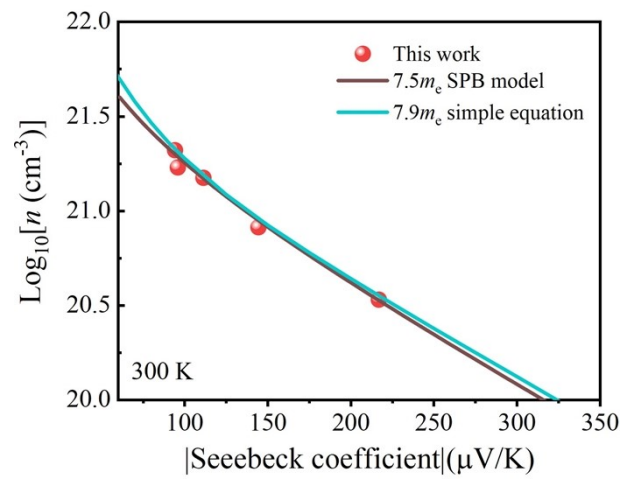
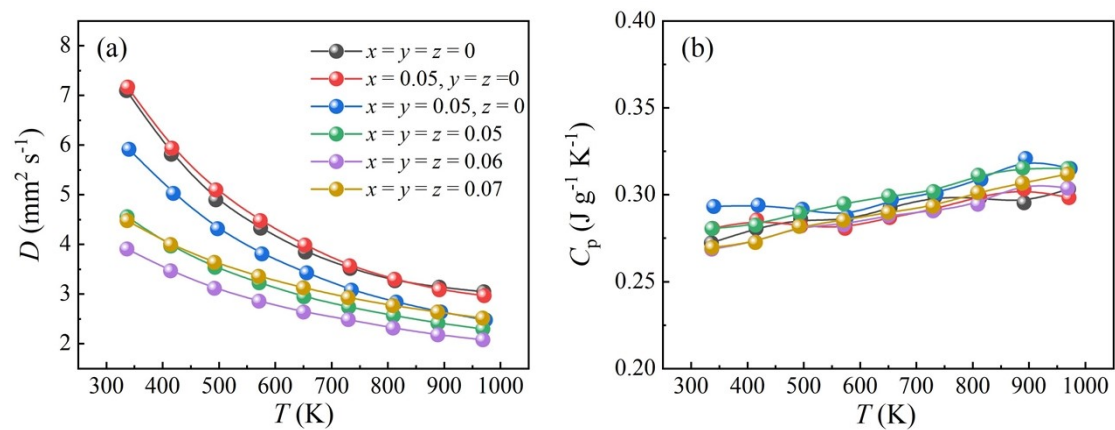
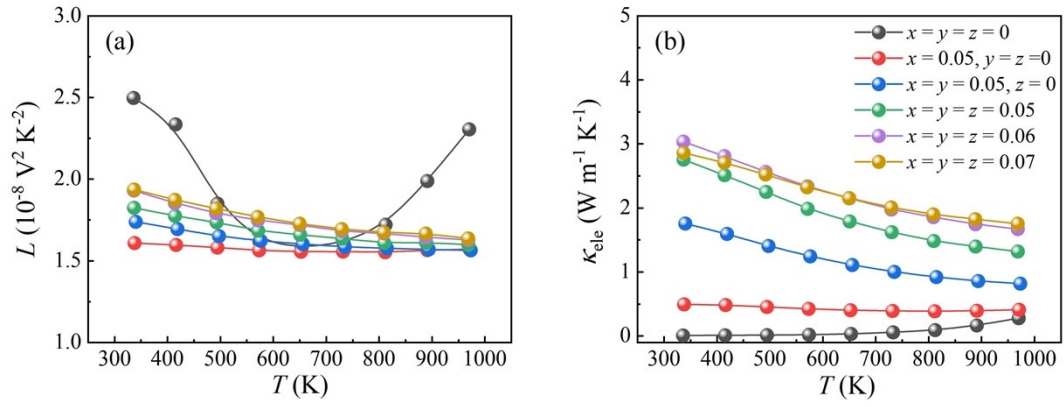


Fig. S5. The  $|S|$ -dependent  $\text{Log}_{10}(n)$  calculated by the simple Equation, the SPB model.



**Fig. S6.** Temperature-dependent (a) thermal diffusivity  $D$  and (b) heat capacity  $C_p$



**Fig. S7.** (a) Calculated Lorentz number using the SPB model and (b) Electronic thermal conductivity for the  $\text{Nb}_{1-x-y-z}\text{Ti}_x\text{Zr}_y\text{Hf}_z\text{FeSb}$  ( $x, y, z = 0, 0.05, 0.06, 0.07$ ) samples.



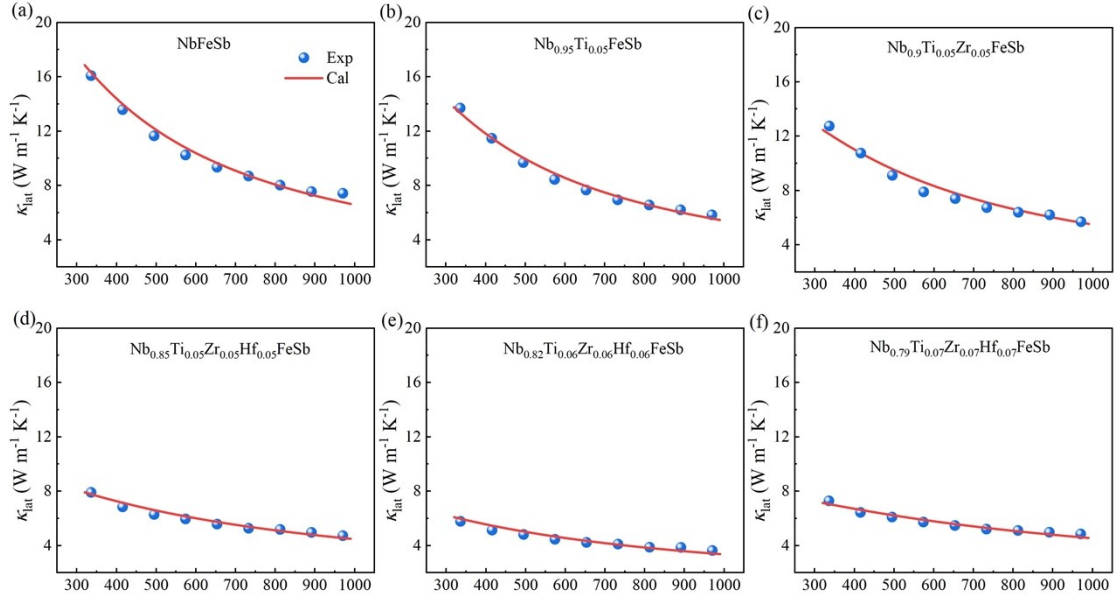


**Fig. S8.** The temperature dependence of lattice thermal conductivity of  $\text{Nb}_{1-x-y-z}\text{Ti}_x\text{Zr}_y\text{Hf}_z\text{FeSb}$  ( $x, y, z = 0, 0.05, 0.06, 0.07$ ) sample and fitting by Debye-Callaway model.

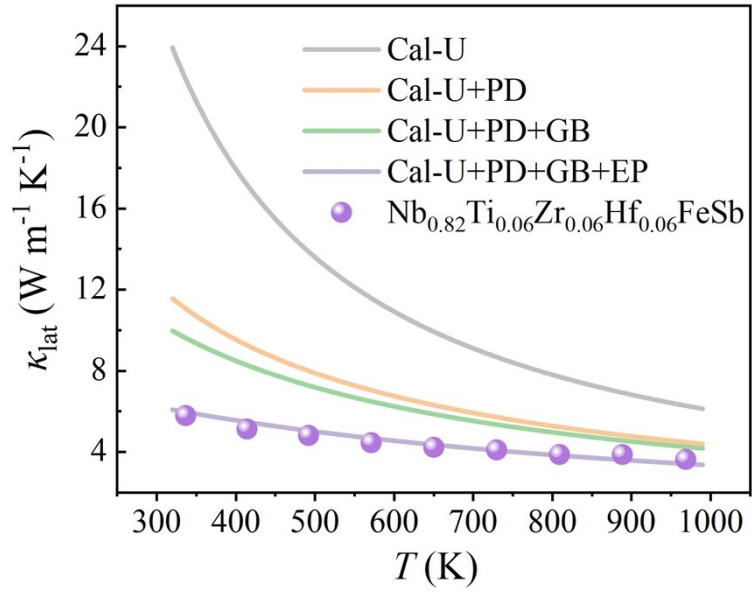


**Fig. S9.** Experimental and theoretical curves for  $\kappa_{\text{lat}}$  of the samples of  $x = y = z = 0.06$ .

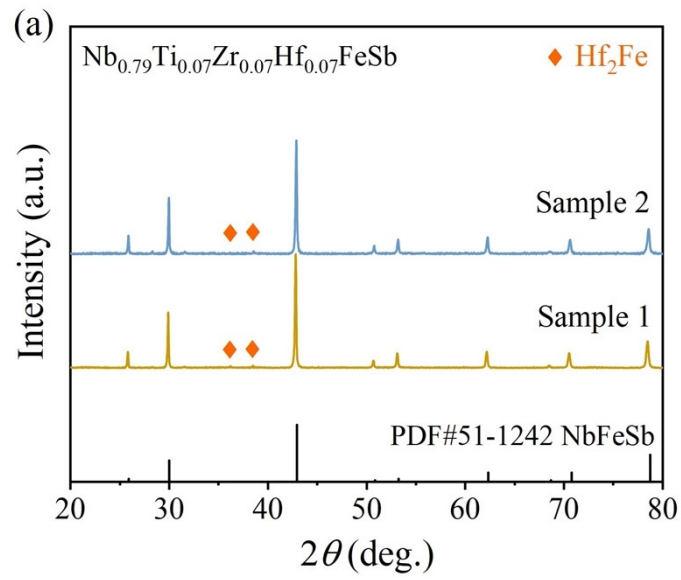


**Fig. S10.** Powder XRD patterns of  $\text{Nb}_{0.79}\text{Ti}_{0.07}\text{Zr}_{0.07}\text{Hf}_{0.07}\text{FeSb}$  sample 1 and 2.

## Supplementary Tables

**Table S1.** The mixing entropy, mixing enthalpy and mixing Gibbs free energy at 1123 K for the Nb<sub>1-x-y-z</sub>Ti<sub>x</sub>Zr<sub>y</sub>Hf<sub>z</sub>FeSb ( $x, y, z = 0, 0.05, 0.06, 0.07$ ) samples.

$x$ - $y$ - $z$  Ti <sub>$x$</sub> Zr <sub>$y$</sub> Hf <sub>$z$</sub> FeSb ( $x, y, z = 0, 0.05, 0.06, 0.07$ ) samples.

$x, y, z$	$\Delta S$ (J mol <sup>-1</sup> K <sup>-1</sup> )	$\Delta H$ (KJ mol <sup>-1</sup> )	$\Delta G$ (KJ mol <sup>-1</sup> )
$x = y = z = 0$	0	0	0
$x = 0.05, y = z = 0$	1.65	0.38	-1.47
$x = y = 0.05, z = 0$	3.28	1.08	-2.60
$x = y = z = 0.05$	4.88	1.74	-3.74
$x = y = z = 0.06$	5.56	1.85	-4.40
$x = y = z = 0.07$	6.19	1.94	-5.01

**Table S2.** The Rietveld refinement details of Nb<sub>1-x-y-z</sub>Ti<sub>x</sub>Zr<sub>y</sub>Hf<sub>z</sub>FeSb ( $x, y, z = 0, 0.05, 0.06, 0.07$ ) samples.

samples.

$x, y, z$	R <sub>p</sub>	R <sub>wp</sub>	$\chi^2$	a (Å)
$x = y = z = 0$	6.19	9.00	4.06	5.9534
$x = 0.05, y = z = 0$	3.12	4.71	4.72	5.9462
$x = y = 0.05, z = 0$	3.14	4.62	4.44	5.9522
$x = y = z = 0.05$	3.00	4.22	4.06	5.9578
$x = y = z = 0.06$	2.80	3.81	2.83	5.9656
$x = y = z = 0.07$	2.92	3.98	2.93	5.9677

**Table S3.** Actual and nominal composition of the Nb<sub>1-x-y-z</sub>Ti<sub>x</sub>Zr<sub>y</sub>Hf<sub>z</sub>FeSb ( $x, y, z = 0, 0.05, 0.06,$

0.07) samples.

Nominal composition	Actual composition	SEM/EDS composition (at %)					
		Nb	Ti	Zr	Hf	Fe	Sb
$x = y = z = 0$	Nb <sub>1.02</sub> Fe <sub>0.98</sub> Sb	34.3				32.8	33.0
$x = 0.05, y = z = 0$	Nb <sub>0.97</sub> Ti <sub>0.05</sub> Fe <sub>0.98</sub> Sb <sub>0.99</sub>	32.4	1.7			32.8	33.0
$x = y = 0.05, z = 0$	Nb <sub>0.92</sub> Ti <sub>0.05</sub> Zr <sub>0.05</sub> Fe <sub>0.99</sub> Sb <sub>0.99</sub>	30.7	1.6	1.8		33.1	32.9
$x = y = z = 0.05$	Nb <sub>0.88</sub> Ti <sub>0.05</sub> Zr <sub>0.05</sub> Hf <sub>0.05</sub> Fe <sub>0.96</sub> Sb	29.6	1.8	1.6	1.7	32.1	33.3
$x = y = z = 0.06$	Nb <sub>0.86</sub> Ti <sub>0.06</sub> Zr <sub>0.05</sub> Hf <sub>0.06</sub> Fe <sub>0.98</sub> Sb	28.5	1.9	1.8	2.1	32.6	33.1
$x = y = z = 0.07$	Nb <sub>0.81</sub> Ti <sub>0.07</sub> Zr <sub>0.07</sub> Hf <sub>0.07</sub> Fe <sub>0.98</sub> Sb	27.1	2.3	2.2	2.4	32.7	33.3

**Table S4.** The fitting parameters for the Nb<sub>1-x-y-z</sub>Ti<sub>x</sub>Zr<sub>y</sub>Hf<sub>z</sub>FeSb ( $x, y, z = 0, 0.05, 0.06, 0.07$ ) samples.

Nominal composition	$\varepsilon$ (G=0)	$A$ ( $10^{-43}$ s <sup>3</sup> )	$B$ ( $10^{-18}$ s/K)	$C$ ( $10^{-16}$ s)
$x = y = z = 0$	1.45	0	1.45	2.50
$x = 0.05, y = z = 0$	30.7	1.01	1.80	2.70
$x = y = 0.05, z = 0$	33.9	2.36	1.65	3.00
$x = y = z = 0.05$	36.3	7.62	1.40	3.20
$x = y = z = 0.06$	28.5	8.37	1.95	3.60
$x = y = z = 0.07$	33.3	11.9	1.10	4.00

**Table S5.** The atom radius and mass of Nb, Ti, Zr, Hf element.

	Nb	Ti	Zr	Hf
Radius (pm)	146	147	160	159
Mass (g cm <sup>-1</sup> )	92.91	47.87	91.22	178.49

**Table S6.** The Young's modulus ( $E$ ) bulk modulus ( $K$ ), and compression modulus ( $E_s$ ) of the Nb<sub>1-x-y-</sub><sub>z</sub>Ti<sub>x</sub>Zr<sub>y</sub>Hf<sub>z</sub>FeSb ( $x, y, z = 0, 0.05, 0.06, 0.07$ ) samples.

$x, y, z$	$E$ (GPa)	$K$ (GPa)	$E_s$ (GPa)
$x = y = z = 0$	261.0	133.7	25.5
$x = 0.05, y = z = 0$	293.0	157.7	38.4
$x = y = 0.05, z = 0$	295.4	164.2	39.2
$x = y = z = 0.05$	267.3	151.9	35.9
$x = y = z = 0.06$	283.1	148.7	31.8
$x = y = z = 0.07$	258.6	142.9	37.5

## Modeling of lattice thermal conductivity

Based on the Debye-Callaway theory, the  $\kappa_{\text{lat}}$  can be expressed as:

$$\kappa_L = \int_0^{\frac{\theta_D}{T}} \kappa_S(x) dx = \frac{k_B}{2\pi^2 v_a} \left( \frac{k_B}{\hbar} \right)^3 T^3 \int_0^{\frac{\theta_D}{T}} \tau(x) \frac{x^4 e^x}{(e^x - 1)^2} dx \quad (1)$$

where  $x = \hbar\omega/(k_B T)$  is the reduced phonon frequency,  $k_B, \hbar, \theta_D$  are the Boltzmann

constant, the reduced Planck constant, the Debye temperature, respectively.  $\tau$  is the sum of the relaxation times from different scattering mechanisms. Here, we mainly focus on the phonon-phonon Umklapp process (U), the point defect scattering (PD), the grain boundary scattering (GB) and the electro-acoustic coupling (EP).

In this work,  $\tau$  is expressed as:

$$\tau^{-1} = \tau_{PD}^{-1} + \tau_U^{-1} + \tau_{GB}^{-1} + \tau_{EP}^{-1} = A\omega^4 + B\omega^2 T \exp\left(-\frac{\theta_D}{3T}\right) + \frac{v}{d} + C\omega^2 \quad (2)$$

Where  $d$  is the grain size and  $v/d$  represents boundary scattering.  $A$  is the pre-factor of point defect (PD) scattering relaxation time due to Ti doping.  $B$  is the prefactor of phonon-phonon Umklapp (U) scattering relaxation time, and  $C$  is the prefactor of electron phonon (EP) scattering relaxation time. For the polycrystalline pure FeNbSb, the dominated phonon scattering mechanism should be the phonon-phonon  $U$  scattering and boundary scattering. Therefore, through fitting the  $\kappa_1$  of polycrystalline FeNbSb, we can obtain the prefactor  $B$  of  $U$  scattering relaxation time. Scattering by point defects arises from both mass and strain differences within the lattice.

In the simple case of alloying:

$$\tau_{PD}^{-1} = \frac{V\omega^4}{4\pi v_a^3} (\Gamma_m + \Gamma_s) \quad (3)$$

Where  $V$  is the volume per atom,  $v_a$  is the average velocity.  $\Gamma_m$  and  $\Gamma_s$  are the disorder scattering parameters of mass and strain field fluctuation, respectively. We can obtain the prefactor  $A$  of point defect (PD) scattering relaxation time, the mass fluctuation ( $\Gamma_m$ ) and strain field term ( $\Gamma_s$ ) parameter are then given by

$$\Gamma_m = \frac{\sum_{i=1}^n c_i \left( \frac{\bar{M}_i}{\bar{M}} \right)^2 f_i^1 f_i^2 \left( \frac{M_i^1 - M_i^2}{\bar{r}_i} \right)}{\left( \sum_{i=1}^n c_i \right)} \quad \Gamma_s = \frac{\sum_{i=1}^n c_i \left( \frac{\bar{M}_i}{\bar{M}} \right)^2 f_i^1 f_i^2 \varepsilon \left( \frac{r_i^1 - r_i^2}{\bar{r}_i} \right)}{\left( \sum_{i=1}^n c_i \right)} \quad (5)$$

where  $\bar{M}_i$  is the average atomic mass of the  $i$  of sublattice, the  $\bar{M}$  is the average atomic mass of the compound,  $f_i$  is the fractional occupant,  $r_i$  is the radius of atom,  $\varepsilon$  is the phenomenological parameter which is a function of the Grüneisen parameter. The mass fluctuation term and the strain field term would be jointly determined by four or five parameters of  $\bar{M}_i, \bar{M}, f_i, r_i, \varepsilon$ , respectively.

For  $\text{Nb}_{1-x-y-z}\text{Ti}_x\text{Zr}_y\text{Hf}_z\text{FeSb}$  ( $x, y, z = 0, 0.05, 0.06, 0.07$ ) samples, the existing phonon scattering sources should be the  $U$  process, boundary, point defects and electron-phonon interaction. The boundary scattering and point defects scattering relaxation times can be calculated independently. Therefore, through fitting the  $\kappa_1$  of corresponding sample, the prefactor  $C$  of the  $EP$  scattering relaxation time can be obtained.

### Calculation of bulk modulus

The bulk modulus ( $K$ ) has been calculated using the following equations:

$$K = \frac{E}{3(1 - 2\nu_p)} \quad (6)$$

$$E = \frac{\rho v_a^2 (3v_l^2 - 4v_t^2)}{(v_l^2 - v_t^2)} \quad (7)$$

$$\nu_p = \frac{1 - 2(v_t/v_l)^2}{2 - 2(v_t/v_l)^2} \quad (8)$$

Where  $E$ ,  $\nu_p$ ,  $\nu_a$ ,  $\nu_l$  and  $\nu_t$  are the Young's modulus, Poisson's ratio, average sound

velocity, longitudinal sound velocity and transverse sound velocity, respectively.